Revista Brasileira de Cartografia
ISSN 1808-0936 | https://doi.org/10.14393/revbrascartogr
Sociedade Brasileira de Cartografia, Geodésia, Fotogrametria e Sensoriamento Remoto

Assessment of Spatial and Temporal Distribution of Clouds in Northeast Brazil (2000 -2019) using MODIS Data

Avaliação da Distribuição Espacial e Temporal de Nuvens no Nordeste Brasileiro (2000 - 2019) utilizando Dados MODIS

Andeise Cerqueira Dutra [1], Egidio Arai [2], Claudia Bloisi Vaz Sampaio [3] e Yosio Edemir Shimabukuro [4]

1 National Institute for Space Research, Remote Sensing Division, São José dos Campos-SP, Brasil. andeise.dutra@inpe.br
ORCID: https://orcid.org/0000-0002-4454-7732
2 National Institute for Space Research, Remote Sensing Division, São José dos Campos-SP, Brazil. egidio.arai@inpe.br
ORCID: https://orcid.org/0000-0003-1994-5277
3 Federal University of Recôncavo da Bahia, Center of Exact and Technological Sciences, Cruz das Almas-BA. claudiabloisi@gmail.com
ORCID: https://orcid.org/0000-0003-1919-0900
4 National Institute for Space Research, Remote Sensing Division, São José dos Campos-SP, Brazil. yosio.shimabukuro@inpe.br
ORCID: https://orcid.org/0000-0002-1469-8433

Recebido: 03.2020 | Aceito: 08.2020

Resumo: O presente estudo tem como objetivo avaliar a distribuição espacial e temporal da cobertura de nuvens no Nordeste brasileiro, mensal e anualmente, a partir de 2000 a 2019, afim de determinar se há um padrão espacial e temporal na distribuição da cobertura de nuvens e se existe um padrão entre a distribuição de cobertura de nuvens em relação à quantidade de chuva. Para isso, foram utilizadas imagens diárias adquiridas para o período analisado pelo sensor MODIS, que incluem a garantia de qualidade (QA) desses dados quanto a cobertura de nuvens (pixel livre de nuvens, com total cobertura de nuvens, ou com mistura de nuvens). Para fins comparativos, dados de QA dos sensores OLI (Landsat-8) e MSI (Sentinel-2) para 2019 foram utilizados. Além disso, foram utilizados dados de chuva adquiridos pelo satélite TRMM, considerando os biomas Amazônia, Mata Atlântica, Caatinga e Cerrado. Os resultados possibilitaram conhecer a distribuição espacial e temporal de imagens livres de nuvens e aqueles com presença de nuvens. Na região Nordeste, os biomas Amazônia e Mata Atlântica são fortemente afetados pela presença de nuvens, enquanto os biomas Caatinga e Cerrado são os menos afetados. Observações anuais não indicam clara evidência sobre a redução na qualidade dos dados em anos mais chuvosos. Enquanto que as observações mensais indicam que, exceto para a Mata Atlântica, nos meses mais chuvosos há redução de ~50% de imagens livres de nuvens. Dessa maneira, os meses mais favoráveis à aquisição de dados por sensores ópticos são no período seco, mais especificamente entre maio e outubro, principalmente no bioma Cerrado. Os resultados apontam a necessidade de aumento na disponibilidade de imagens orbitais livres de nuvens na região, sobretudo nos biomas Amazônia e Mata Atlântica, visto que isso se torna um fator limitante para o mapeamento e monitoramento de uso e cobertura da terra dessa região principalmente quanto menor for a resolução temporal do sensor utilizado.
Palavras-chave: MODIS. Sentinel-2. Landsat-8. Precipitação. Biomas. Sensoriamento Remoto.

Abstract: The present study aims to assess the spatial and temporal distribution of cloud cover in Northeast region of Brazil, monthly and annually, from 2000 to 2019, in order to determine if there is a spatial and temporal pattern in the distribution of cloud cover and if there is a pattern between the distribution of cloud cover in relation to the amount of rainfall. For this, daily images for the analyzed period by the MODIS sensor were used, which include the quality assurance (QA) of the data produced (clear pixel, pixel with total cloud cover, or pixel mixed with clouds). For comparative purposes, QA data from OLI (Landsat-8) and MSI (Sentinel-2) sensors for 2019 were used. Besides that, rainfall data from TRMM satellite were used considering the Amazon, Atlantic Forest, Caatinga and Cerrado biomes. The results made possible to know the spatial and temporal distribution of the cloud free images and those with presence of cloud. In the Northeast region, the Amazon and Atlantic Forest biomes are strongly affected by the presence of clouds, while the Caatinga and Cerrado biomes are less affected. Annual observations did not indicate clear evidence about the reduction in the data quality in the wettest years. While monthly observations indicated that in the wettest months there was a ~50% reduction of cloud free images. So, the most favorable months for data acquisition by optical sensors are observed in the dry period, specifically between May and October, mainly in the Cerrado biome. The results point to the need to increase the availability of temporal orbital images in the region, especially in the Amazon and Atlantic Forest biomes, as it becomes a limiting factor for land use and land monitoring in that region mainly to the lower temporal resolution of the used sensor.
Keywords: MODIS. Sentinel-2. Landsat-8. Precipitation. Biomes. Remote Sensing.

1 INTRODUCTION

The Northeast region of Brazil (NEB) covers about 18% of the country and comprises the most populous semiarid region in the world (MARENGO; CUNHA; ALVES, 2016). The region has been strongly affected by environmental problems related to anthropic pressure, as land degradation, and extreme climate events, being one of the world's most vulnerable areas (SANTOS et al., 2011; MARENGO; CUNHA; ALVES, 2016; CONFALONIERE et al., 2014; CUNHA et al., 2018). Thus, in recent years there have been an increase in research efforts to know the extent, intensity, and impacts of these factors in this region (da SILVA et al., 2017; TOMASELLA et al., 2018; BRITO et al., 2018; MARIANO et al., 2018; BARBOSA et al., 2019; dos SANTOS et al., 2020).

To achieve the goals mentioned above, many efforts require to know patterns, characteristics of land-use and land-cover (LULC), also to quantify rates of changes in a large-scale temporal and spatial data of the Earth's surface (ASNER, 2000). In this manner, over the past decades remote sensing products have become an important up-to-date source of Earth's surface information due to the possibility of acquiring data over large geographic extensions and cost-effective, also due to the long-term historical data, contributing for a huge monitoring and mapping efforts (SANO et al., 2010; ZALLES et al., 2019). Such products have been allowing a better understanding of ecological, biogeochemical, and atmospheric processes on global to local scales (ASNER, 2000), and also providing support to decision-makers for planning and public policies.

Currently, there are several satellite-based products widely available with different spectral, temporal and spatial resolutions, which have allowed the developing and increasing the number of monitoring and mapping systems. In Brazil, for example, researches have been conducted on mapping LULC classes or environmental disturbances at a national scale, e.g. the *MapBiomas* project (MAPBIOMAS, 2020) which provides LULC maps; and the *Fire Monitoring Program* managed by *INPE* (*National Institute for Space Research*) (INPE, 2018). Or even at a biome or regional scale, e.g. the *INSA (National Institute for Semiarid)* which provides a spatial analysis of desertification in the Brazilian semiarid (INSA, 2020); also the *DETER (Warning system)* (INPE, 2020), *PRODES (Deforestation Monitoring by Satellite Project*) (INPE, 2020), and *SOS Mata Atlântica* (SOSMA, 2020) projects which were developed to detect deforestation and forest degradation, and it covers parts of NEB.

However, when dealing with images generated from remote sensing, the radiation detected by the sensor is resulted of the electromagnetic radiation interactions of multiple targets response, also the atmospheric elements (SHIMABUKURO; SMITH, 1995). Cloud formation is an atmospheric element and, in the remote sensing user's community, cloud cover is defined as the fractional area covered by clouds observed from satellites, characterized by higher reflectance (ACKERMAN et al., 1998; YOUSEF et al., 2020) and commonly accompanied with corresponding shadow. Then the presence of cloud cover causes changes in reflectance values, preventing the analysis and affecting the results (LU et al., 2007). In this sense, the absence of clouds and shadows is crucial for most time series applications of optical data, being fundamental to know, a priori, their spatial and temporal distribution (RUDORFF et al., 2010; CLAVERIE et al., 2018).

Particularly, most of the efforts that aims LULC mappings have used a combination of both medium spatial resolution and relatively long re-visiting capability satellite data (e.g., Landsat satellite series) to be an advantageous product in detecting LULC changes. However, as indicated by Asner (2001) in the Brazilian Amazon basin and by Sano (2007) in the Brazilian Cerrado, monthly observation data could be highly unavailable imposed by cloud cover. In this manner, to increase the availability of temporal images once applications needed near-daily imagery at medium spatial resolution, monitoring or warning systems have been conducted combining data provided by different sensors, e.g. CBERS (China – Brazil Earth Resources Satellite) and IRS (Indian Remote Sensing) by *DETER project*, or CBERS and Landsat series by the *SOS Mata Atlântica project*.

Although the significantly importance to stablish and achieve efforts to analyze, map and monitor anthropogenic and climate effects in the NEB, few studies have addressed the estimates of cloud cover imagery from optical satellite data in this region. In this context, the present study aims to assess the spatial and temporal distribution of cloud cover in the NEB, monthly and annually, from 2000 to 2019 period to answer the following questions: (i) is there a spatial and temporal pattern in cloud cover distribution over NEB?; and (ii) is there a pattern between estimates of cloud cover in relation to the amount of rainfall, once clouds play an important role on controlling precipitation?

For this purpose, it was used the MOD09GA product dataset from the Moderate Resolution Imaging Spectroradiometer (MODIS) sensor, currently onboard Terra and Aqua platforms, with large swath view and polar orbit that provides daily images (JUSTICE et al., 2002; KRAATZ; KHANBILVARDI; ROMANOV, 2017) to answer the question (i). For comparative purposes, the datasets from Landsat-8/Operational Land Imager (OLI) and Sentinel-2A and -2B/ MultiSpectral Instrument (MSI) were used. To answer the question (ii), rainfall data recorded by the Tropical Rainfall Measuring Mission (TRMM) satellite was used.

In summary, the following content of this article is divided into four sections. Section 2 provides a general description of the study area. In Section 3 are presented the dataset and methodological approach adopted to achieve the objectives. Section 4 presents the results and discussion, and also a brief perspective related to platforms/sensors and methods to improve the availability of images for mapping and monitoring in remote sensing applications. Finally, Section 5 presents the conclusions. This paper is an extended version of Dutra et al. (2019), presented in IX Brazilian Symposium on GeoInformatics (GEOINFO 2019).

2 STUDY AREA

The study area corresponded to the Northeast region of Brazil (NEB), situated in the equatorial zone bounded by latitudes 1º N to 18º S and longitudes 33º W to 49º W (Figure 1). This area comprises approximately 1.55 million km² (~18.27%) of the national territory, which includes the states of Alagoas, Bahia, Ceará, Maranhão, Paraíba, Pernambuco, Piauí, Rio Grande do Norte and Sergipe (IBGE, 2016). Four biomes encompass the region: Amazon (Am) and Atlantic Forest (At) (tropical rainforests; 7.36% and 10.71% respectively, of NEB), Caatinga (Ca) (seasonally dry tropical savanna, 52.52%), and Cerrado (Ce) (tropical savanna, 29.41%).

The NEB is characterized by a heterogeneous and diversity landscape, hosting an impressive fauna and floristic biodiversity (DE ALBUQUERQUE et al., 2012). In addition, the region has a potential of agricultural production, for example, 57% of the territory was quantified as pasture and cropland in 2010 (VIEIRA et al., 2013). However, the pressure over protected areas, inadequate management, deforestation and forest degradation ally to decrease of precipitation bring negative outcomes as the habitat loss and biodiversity reduction, and also very large disturbed areas undergoing desertification event (SANO et al., 2010; de ALBUQUERQUE et al., 2012).

The spatio-temporal distribution of rainfall is characterized as variable and irregular (CUNHA; ALVALÁ; NOBRE, 2015) and the annual total accumulated ranges approximately between 2000 mm/year and 700 mm/year among the biomes, being most rainfall caused by low clouds (Figure 1) (KOUSKY, 1979; ALVARES et al., 2013, PALHARINI; SANTOS; VILA, 2017). The high rainfall variability is induced by different meteorological systems acting in this region, also breezes, winds, and topography influences (MOLION; BERNARDO, 2002).

Figure 1 shows the location of NEB in South America (inset figure), also the four biomes which encompass the region corresponding to Amazon (green), Atlantic Forest (light green), Caatinga (yellow), and Cerrado (orange), including the nine states. Figure 1 also indicates the annual total accumulated rainfall for each biome, being the maximum total accumulated observed in Amazon and the minimum total accumulated observed in Caatinga.

Figure 1 – Location of the Northeast region of Brazil, with four biomes: Amazon, Atlantic Forest, Caatinga and Cerrado, characterized by different rainfall ranges.

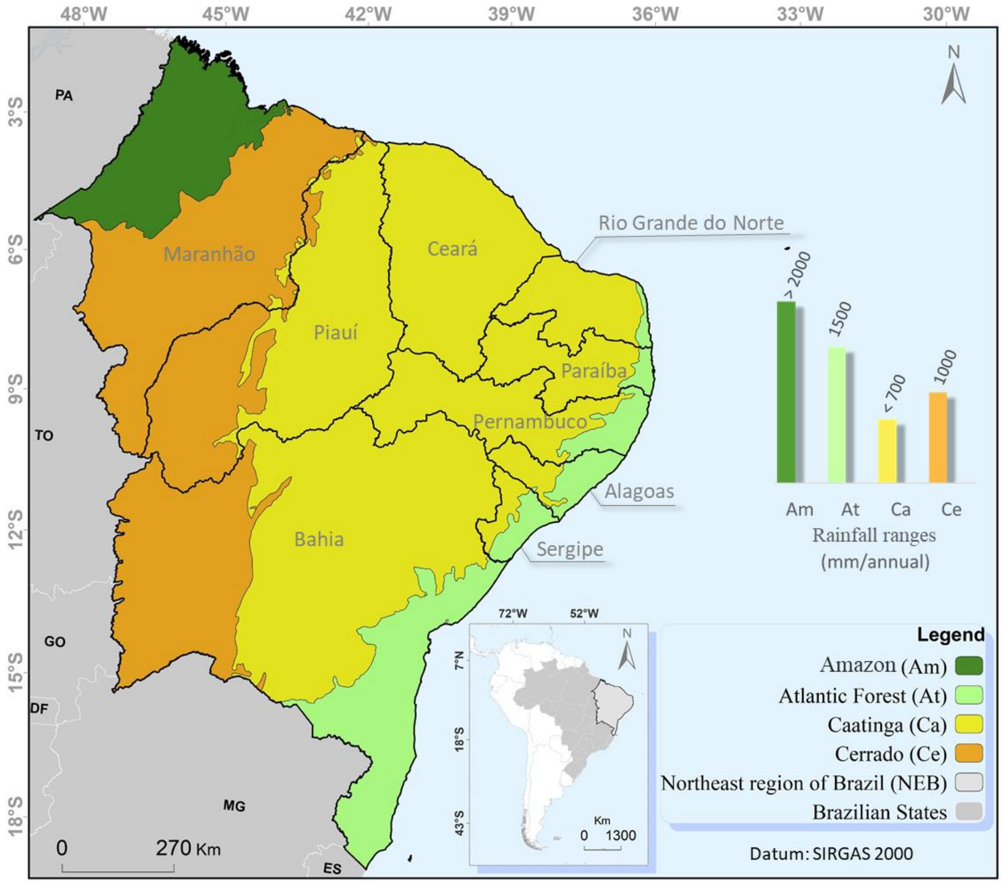

Source: The authors (2020).

3 MATERIALS AND METHODS

This section presents the description of the datasets of MODIS sensor and TRMM satellite comprising the entire time series under study (2000 to 2019) at NEB, as well as the datasets from the OLI and MSI sensors used as a comparison in 2019 year. In addition, the methodology used in data processing and analysis to answer questions (i) and (ii) is presented.

3.1 Data description

3.1.1 QUALITY ASSURANCE MODIS DATA

The MODIS sensor offers several ready-to-use products such as surface reflectance, surface temperature, net primary productivity and vegetation indices (BORGES; SANO, 2014). Among the products, the MOD09GA – version 006 provides daily surface reflectance images at 500-meter spatial resolution, with atmospheric and geometric corrections considering the nadir adjustment to avoid distortion due to data compression. This dataset includes seven spectral bands, which are located in the visible, near-infrared, and middle-infrared wavelength regions. In addition, the product provides a quality band containing information pixel-by-pixel on the conditions of the data produced (DIDAN et al., 2015; VERMOTE; WOLFE, 2015). This band is denominated Quality Assurance (QA), available in MODIS products, developed and implemented to verify the quality of the long-term surface reflectance data records (ROY et al., 2002).

The QA band on MODIS products is presented in numeric values (bits), which can only assume binary values, i.e. 0 and 1. They are meant as a brief summary of quality control aspects of each pixel, with 'QA = 00' meaning the best possible atmospheric correction, i.e. a clear pixel, and any other value indicates errors or problems, e.g. cloudy and mixed pixels, serving as a flag to check others quality reasons than clouds and

 DOI: http://dx.doi.org/10.14393/rbcvxxnx-xxxx

shadow in more detail (VERMOTE; WOLFE, 2015). Used effectively, the QA band support to improve the analysis or selection data purposes, being as a mask to remove non ideal quality pixels in remote sensing applications, once the results might not show the true surface characteristics if such pixels were included (BRANDT et al., 2016; ROY et al., 2019).

In this work, all daily QA band from MOD09GA product was acquired for the period from 2000 to 2019, covering the entire NEB which corresponds to the area covered by MODIS land tiles H13V10, H13V09, H14V10 and H14V09 (WOLFE; ROY; VERMOTE, 1998). This dataset was chosen due to its temporal resolution that increases the probability of finding pixels without clouds, providing a general distribution in the NEB. All dataset was accessed and processed on Google Earth Engine (GEE) platform (GORELICK et al., 2017).

3.1.2 TROPICAL RAINFALL MEASURING MISSION DATA

To answer the question about the patterns between estimates of quality data in relation to the amount of rainfall in the NEB, data derived from the Tropical Rainfall Measuring Mission (TRMM) satellite product 3B43-V7, were obtained for the same period of this study. This product is available at a 0.25 degrees (approximately 27.5 x 27.5 km or 760 km²) spatial resolution, covering the globe between latitudes 50º N to 50º S, and distributed in HDF format – Hierarchical Data Format (TRMM, 2011).

The dataset provides rainfall estimates in millimeters per hour for each pixel, in a monthly temporal resolution. This dataset was chosen due to its temporal resolution, and validations performed for the NEB showed a significant high correlation (> 0.75) and agreement between the data estimated by the product and those observed in the field by rainfall gauges (SANTOS et al., 2015; SOARES; PAZ; PICCILLI, 2016). All datasets were accessed in NASA Services Website (https://giovanni.gsfc.nasa.gov/giovanni/) (ACKER; LEPTOUKH, 2007) and processed on RStudio under R programming language (Team R, 2015; R Core Team, 2020).

3.1.3 AUXILIARY DATA

For comparative purposes, a free available Landsat-8 OLI and Sentinel-2 (both 2A and 2B satellites) MSI datasets were used due to their higher spatial resolution compared with MODIS dataset, and also differences in the temporal resolutions.

The Landsat-8 OLI has nine reflective wavelength bands distributed in the visible, near and middle infrared regions, provided in 30-meter spatial resolution and a 16-day temporal resolution (ROY et al., 2019). The Sentinel-2 MSI has 13 reflective wavelength bands distributed in the visible, near and middle infrared regions provided mostly in 10-meters or 20-meters spatial resolutions, and a global average revisit interval of ~4-days when both satellites are combined (DRUSCH et al., 2012; LI; ROY, 2017). Both products have a QA band implemented.

In this work, OLI and MSI datasets were acquired only for the 2019 year covering the NEB, once products have differences in time-series due to the launched year of each satellite. The datasets were also accessed and processed on GEE platform.

3.2 Methodology

Considering that the QA MODIS description is provided in bits (totalizing 16-bits), and the pixel values in the QA MODIS band is represented in decimal values, it required a translation into binary form to be used effectively (Figure 2). Each bits group provides parameters of quality status. In this case, the first two bits from right to left (highlighted in red in Figure 2), for example, are related to the parameters of cloud status and provide four different binary combinations (00, 01, 10, and 11) corresponding to a pixel quality. The first three combinations can be described as good quality, cloudy, and mixed pixels, and the fourth combination is the non-produced pixels due to other reasons than clouds (Table 1) (VERMOTE; WOLFE, 2015). Then, only the first three combinations were selected for this study, disregarding the non-produced pixels.

The mentioned binary combinations allowed to account the number of pixels described as in clear, cloudy, and mixed conditions and then, to calculate the average for each quality condition per month and year. The average was calculated considering the number of days per month, in leap and non-leap years, and also considering that available MODIS images started in March 2000. To represent the results numerically in a plot, a unique average value considering the total spatial extension of each biome was extracted. In this manner, the discussion was divided into four regions, corresponding to the Amazon, Atlantic Forest, Caatinga, and Cerrado biomes to answer the question (i).

The same methodological approach was also applied in the QA bands from Landsat-8 and Sentinel-2 datasets, but only extracting the binary combination described as a clear condition for comparison purposes. In this manner, the QA bands from both satellites were used to account the number of cloud-free observations in the year. Finally, surface reflectance images provided by MODIS, OLI, and MSI sensors in a sample area located in NEB (bounded by latitudes 13º N to 14º S and longitudes 39º W to 40º W) were used to demonstrate the application of the QA bands as a cloud bitmask and the differences to detect clouds between products.

Figure 2 – Example of one-pixel value in the QA MODIS band and the selection of correspondent binary combination related to cloud status.

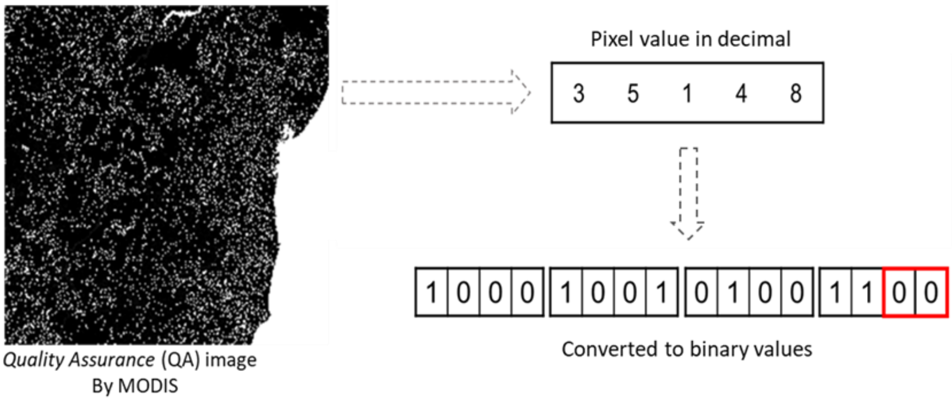

Source: The authors (2020).

Table 1 – Image parameter of quality data and their respective description.

Bit	Parameter	Binary Combinations	Description
0 –1	Cloud status bits	00	Produced with good quality (clear)
		01	All cloudy
		10	Mixed with clouds
		11	Not produced due to the reasons other than clouds

Source: Didan et al. (2015).

Related to TRMM dataset, millimeters per hour (mm/hour) values were multiplied by the number of hours each month, considering leap and non-leap years, to obtain monthly total accumulated rainfall estimates (mm/month) pixel-by-pixel. Then, from this result, the rainfall average by month and year was calculated considering the time-series under study (2000 to 2019). Finally, to answer the question (ii), a unique average value considering the total spatial extension of each biome was extracted aiming to plot numerically the results with QA MODIS by month and year.

4 RESULTS AND DISCUSSION

Considering the time-series from 2000 to 2019 of the QA MODIS band, the average of clear images observations is approximately 16, 19, 35 and 41%, in Amazon, Atlantic Forest, Caatinga and Cerrado biomes, respectively (Table 2) in the NEB. In other words, the Amazon and Atlantic Forest biomes had more than 60% of the image pixels classified as cloudy and mixed conditions by the QA MODIS, representing less than ~67 days of clear image pixels during the year, being the regions most affected by cloud cover. The increasing in clouds in coastal regions, as observed e.g. encompassing the Atlantic Forest, could be explained by the fact that winds are generally perpendicular to the coast and carry a lot of moisture from the ocean to the continent, contributing to the formation of shallow clouds (PALHARINI; SANTOS; VILA, 2017). On the other hand, the lowest cloud cover could be observed over central and west regions, where are located the Caatinga and Cerrado biomes, achieving ~127 daily images/year in clear condition in both biomes.

Table 2 – Average annual and standard deviation percentages of pixel quality condition in relation to cloud status: 2000-2019.

Biome	**Average annual and standard deviation of pixel quality condition (%)**		
	Clear	**Cloudy**	**Mixed**
Amazon	15.62 ± 2.38	57.80 ± 3.04	10.45 ± 0.94
Atlantic Forest	18.97 ± 1.97	58.70 ± 3.32	10.78 ± 0.96
Caatinga	35.47 ± 3.20	43.39 ± 3.28	8.30 ± 0.43
Cerrado	40.97 ± 3.37	39.02 ± 3.04	7.08 ± 0.44

Source: The authors (2020).

Figures 3 and 4 show the comparison between the annual average of the QA MODIS and the annual average rainfall estimates. It was observed a slight decrease in the average of days described as cloudy pixel when also there was a decrease in the average of rainfall. In years identified with negative rainfall anomalies characterized by a moderate El Niño event in 2009/2010 at the Amazon (ARAGÃO et al., 2018), for example, the average of image pixels described as in clear condition was higher (~18%) when compared to 2000/2001 year characterized by a La Niña event (~11%) (Figure 3a). This pattern is also observed in the others biomes, with the highest average of clear image pixels at Atlantic Forest (~22%), Caatinga (~39%) and Cerrado (~44%) biomes in the very strong 2015/2016 El Niño event compared to the whole period analyzed (Figures 3b, 4a, and 4b). However, there is no clear evidence of this pattern in all rainfall anomalies years.

Figure 3 – Annual average of QA MODIS and annual average rainfall estimates, from 2000 to 2019 years, encompassing the Amazon and Atlantic Forest biomes.

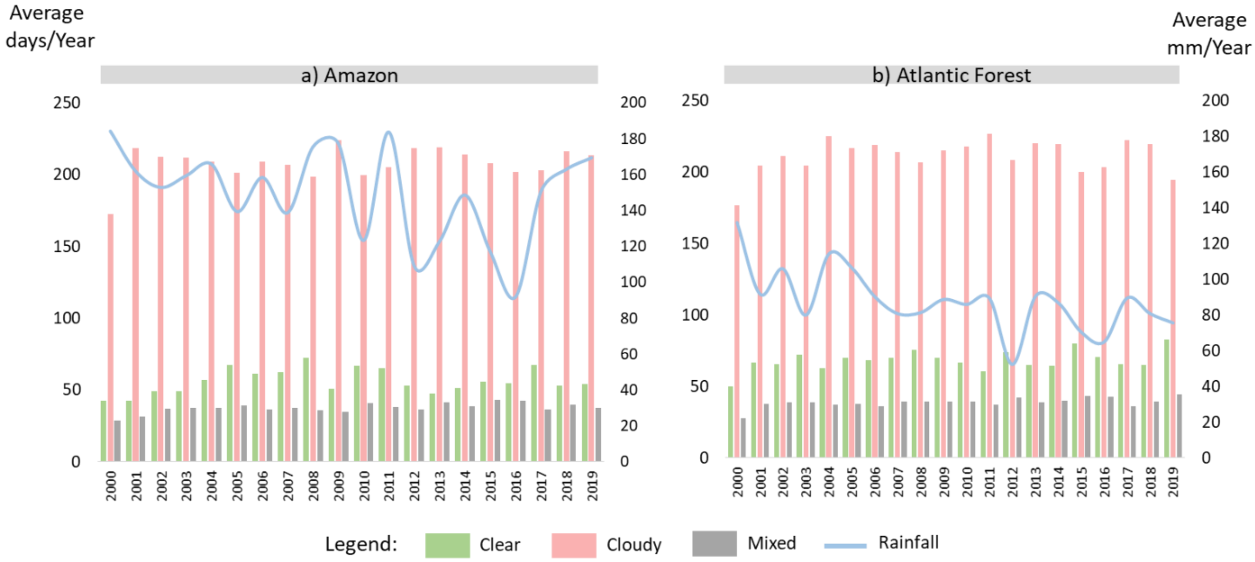

Source: The authors (2020).

 DOI: http://dx.doi.org/10.14393/rbcvxxnx-xxxx

Figure 4 – Annual average of QA MODIS and annual average rainfall estimates, from 2000 to 2019 years, encompassing the Caatinga and Cerrado biomes.

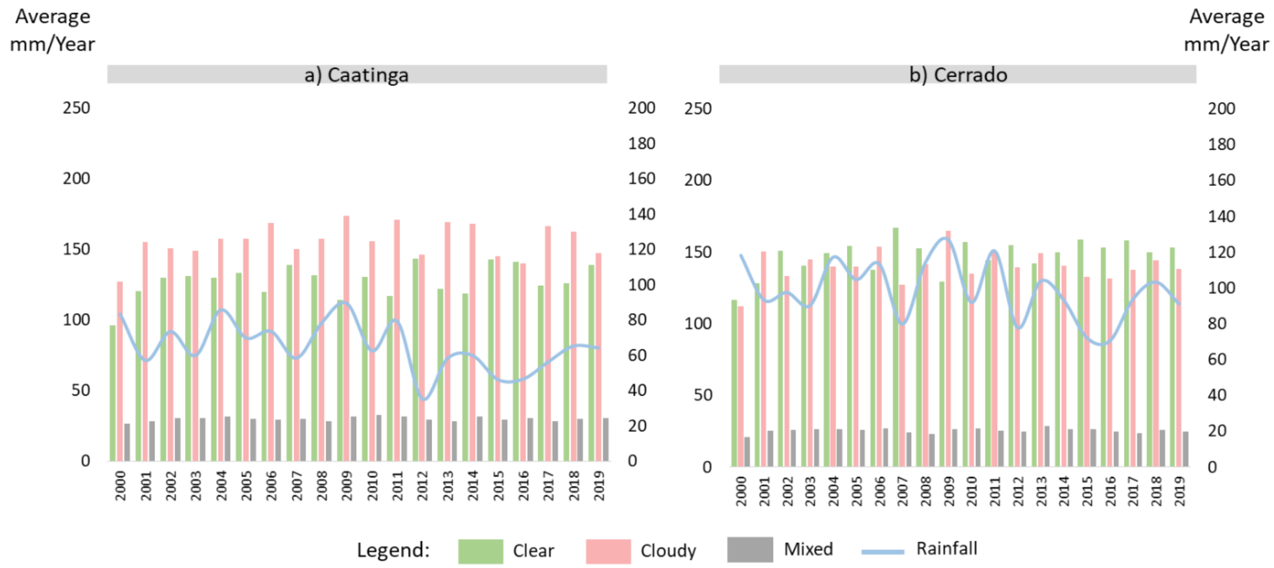

Source: The authors (2020).

Figure 5 shows the comparison between the monthly average of the QA MODIS and the monthly average rainfall estimates. The Amazon, the biome with the lowest availability, on average, of clear images pixel (5 images/month), presents also the highest average of rainfall (~147 mm/month) (Figure 5a). Conversely, Caatinga presents the lowest average rainfall (~65 mm/month) and is the second biome with the highest availability of clear images pixel (11 images/month on average) (Figure 5c). The Atlantic Forest showed an average of 6 images/month per pixel in clear conditions and an average in rainfall of 88 mm/month (Figure 5b), while the Cerrado showed an average of 12 images/month per pixel in clear conditions with an average in rainfall of 98 mm/month (Figure 5d).

The highest average of mixed and cloudy conditions follows the trend of increasing monthly rainfall, i.e. mostly the beginning and end of the year, during the wet season. Conversely, the highest amount of clear condition is most predominant from May to October in Amazon (Figure 5a), Caatinga (Figure 5c) and Cerrado (Figure 5d) during the dry season. On average, only 2 images/month per pixel in clear conditions is available in the Amazon during the peak of the wet season, increased to 9 images/month in the driest month. Also in this sense, increases of 6 to 14 images/month in the Caatinga biome, and 6 to 21 images/month in the Cerrado biome was observed. No distinguished patterns within the Atlantic Forest biome were observed, presenting an average of 6 images/month per pixel in clear condition during the year. (Figure 5b).

In relation to the patterns between QA MODIS and rainfall analysis, it is important to notice that uncertainties may be associated with the heterogeneity of the landscape within a 250-km² cell of the MODIS product and within 760-km² cell of the TRMM product. The lower spatial resolution and the higher differences between both datasets may not detect slightly environmental changes, either overestimate or underestimate the rainfall amount.

 DOI: http://dx.doi.org/10.14393/rbcvxxnx-xxxx

Figure 5 – Monthly average of QA MODIS and monthly average rainfall estimates, from 2000 to 2019 years, encompassing the four biomes.

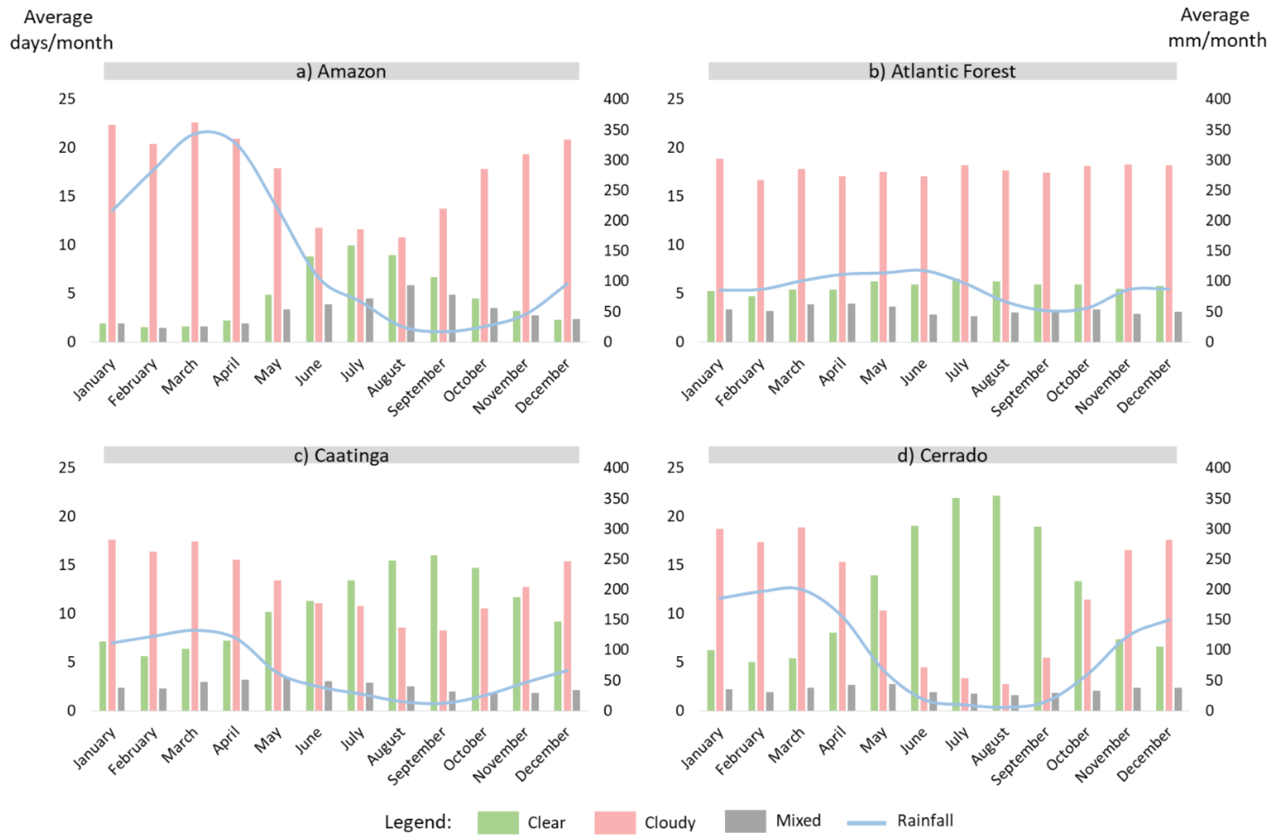

Source: The authors (2020).

Figure 6 shows the monthly spatial and temporal variability of pixels considered as a clear condition in the entire period of study. The wettest part of the year, comprising the months of December through April, is characterized by the most problematic time period, with the lower percentage of clear acquisitions by MODIS for a largely area in NEB. The most affected region is founded in the Amazon and Atlantic Forest, especially in the states of Maranhão, Piauí and Ceará, with a minimal area covering more than 20% and less of 40% observations (representing less than 146 images by year). In Caatinga and Cerrado, only a minimal area encompassing the biomes present more than 40% of clear observations. In the months of June, July, August, and September is observed the increase in the availability of better-quality data for the entire region, being the better suited for obtaining orbital imagery from optical sensors. In particular, the western boundaries of NEB experienced a percentage of 80 – 100% of clear conditions (July and August), in a well-established agricultural producer region in the Bahia State, and the south of Piauí and Maranhão States, the most recent agricultural expansion in Brazil inserted on the agricultural frontier locally known as the MATOPIBA (acronym of Maranhão,Tocatins, Piauí, and Bahia States).

Many activities in NEB need to be monitored due to the impact on landscape fragmentation, soil erosion, water resources, loss of biodiversity, agricultural management, disaster response, ecological process as vegetation phenology, and changes in the storage and flow of carbon emissions. In this manner, numerous studies and efforts have documented the need for more frequent observations associated with better medium spatial resolution for better monitoring studies (SANO et al., 2007; CLAVERIE et al., 2018).

However, currently high and medium spatial resolution sensor products may be limited by the lower frequency of revisit (HILKER et al., 2009; LI et al., 2017), decreasing the potential for using a “single class” sensor. For example, Landsat sensors can have a maximum of 23 observations in a year, while up to 70 from the Sentinel-2A and 2B satellites sensor, disregarding overlaps (PARENTE et al., 2019; CASSOL et al., 2020). Nonetheless, considering the temporal distribution of cloud and cloud shadow cover, not all these observations may be available as valid with clear condition.

 DOI: http://dx.doi.org/10.14393/rbcvxxnx-xxxx

Figure 6 – Monthly average of the spatial distribution of images described as clear condition by QA MODIS from 2000 to 2019 in percentage and approximate number of scenes.

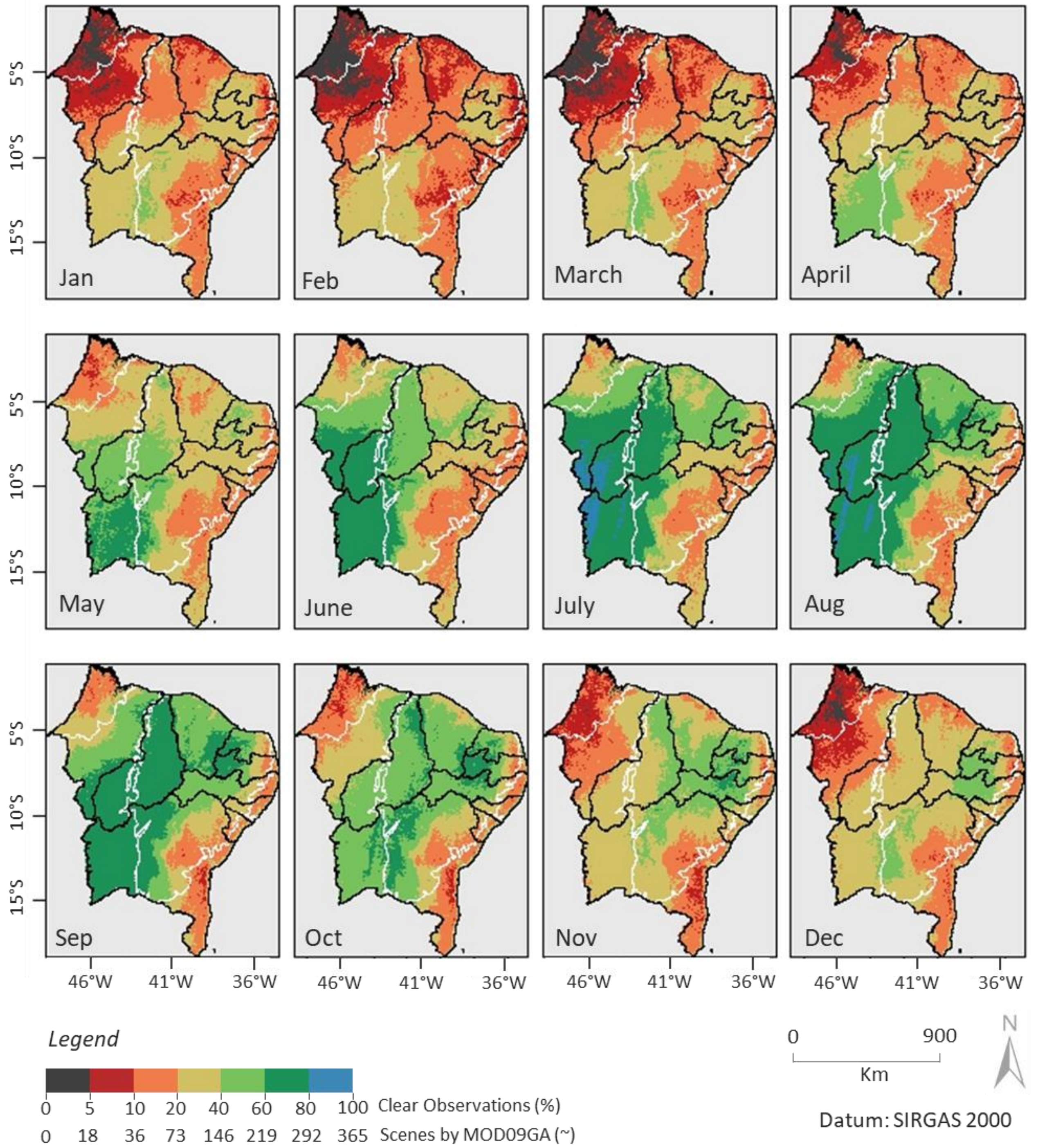

Source: The authors (2020).

Figure 7 provides the spatial and temporal distribution of the cloud–free and cloud shadow-free images pixels over the NEB in 2019 year from Landsat-8 OLI (Figure 7a) and Sentinel-2 MSI (Figure 7b) observations using the data provided by the quality assurance of both products. It was observed the same patterns of the QA MODIS dataset, with less valid observations encompassing the Amazon and Atlantic Forest biomes. In these regions, less than ten images from OLI were available during the year, while a substantial increase from Sentinel-2 satellites was noted. Comprising the Amazon, Asner (2001) founded an annual probability of less than 10% in cloud-free images from Landsat, and the availability of data could not be sufficiently for monitoring studies.

In the central region of NEB, comprising the Caatinga and Cerrado biomes, there is an increase of available images in valid conditions, up to ten images/year from OLI, and up to fifty images/year from MSI

 DOI: http://dx.doi.org/10.14393/rbcvxxnx-xxxx

sensor. However, the probability to find Landsat imagery containing less than 10% of cloud cover decreases during the wettest period in the regions covering Cerrado biome (SANO et al., 2007).

Figure 7 – Annual spatial and temporal distribution of images described as valid condition by QA Landsat-8 OLI (a) and Sentinel-2A and -2B MSI (b) in 2019 year, in percentage and approximate number of scenes.

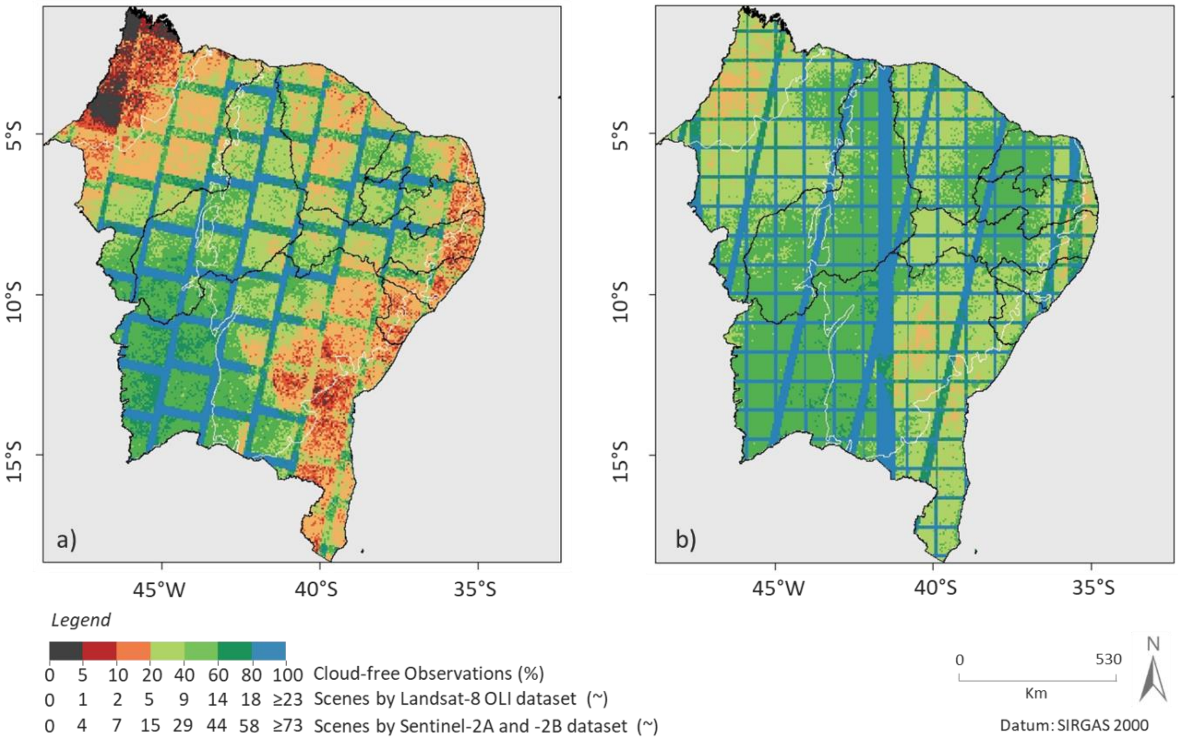

Source: The authors (2020).

The valid dataset of the proposed study was based on the implemented quality assurance algorithm for each product. Nonetheless, it means that the algorithms do not perform with equal accuracies (Figure 8). For example, the current Sentinel QA data as cloud bitmask product still performs poorly to detect cloud and cloud shadow (COLLUZZI et al., 2018) (Figure 7c), resulting in overestimates of valid pixels in the present analysis, while the Landsat algorithm fits well (Figure 7b).

Figure 8 – QA bands used as a bitmask to remove cloud and cloud shadow in surface reflectance images of MODIS (a), Landsat (b), and Sentinel-2 (c), considering the closest date between images.

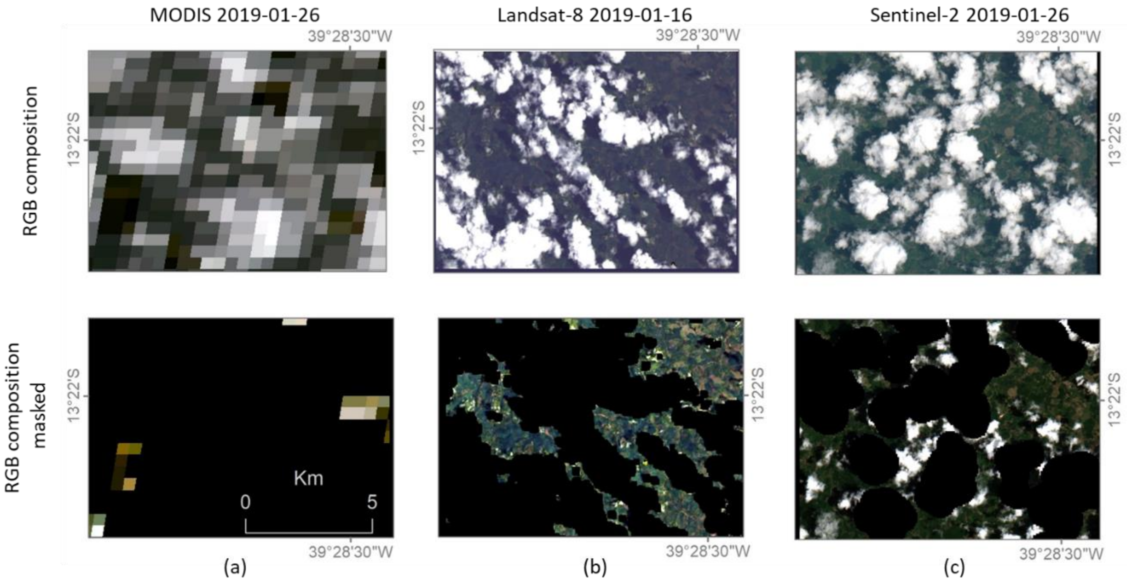

Source: The authors (2020).

4.1 Perspectives for mapping and monitoring studies

Highlighting the efforts and demands for land monitoring, deforestation ranking estimates in the Atlantic Forest by the SOSMA (2020) shows that the Bahia State occupies the first place in this deforestation ranking between 2016/2017 period. In addition, the 2017/2018 period reveals that between the five states those still maintaining unacceptable rates of deforestation, two encompasses in NEB: Piauí (2,100 ha of deforestation) and Bahia (1,985 ha) States. Non-less aggravating, in Cerrado biome the DETER system (corresponding to may/2020 observation), pointed that the five most deforested municipalities are in NEB: Balsas/Maranhão (174 Km²), Formosa do Rio Preto/Bahia (166 Km²), Luis Eduardo Magalhães/Bahia (74 km²), Jaborandi/Bahia (71 km²), and São Desidério/Bahia (69 km²) (ASSIS et al., 2019; INPE, 2020). In these operational systems, two satellite datasets are considered to map the Atlantic Forest and Cerrado biomes as cited in section 1. Updated official deforestation estimates were not found for the Caatinga biome.

In this manner, the existing systems cited above show the importance to establish monitoring efforts to know the extension and rates of LULC changes, for example. To achieve these goals with remote sensing requires cloud-free images frequently, being highly recommended to know, a priori, the spatial and temporal distribution of cloud cover derived from satellite images to subsidize the planning of land monitoring.

Then, as alternative to improve temporal availability of images from orbital sensors, the increasing number of Earth observation satellites providing free imagery and the increased availability of cloud computing environments (e.g. GEE, Amazon Web Services) that provide on up-to-date processing and analysis, has been allowing researchers to develop capabilities for working with a large volume datasets, also combining data from two or more different sensors (LI; ROY, 2017; CLAVERIE et al., 2018; ROY et al., 2019). Moreover, potential alternatives including the synergisms development between the synthetic aperture radar (SAR) and multiple optical platforms/sensors has been conduct and should be considered in the NEB studies.

5 CONCLUSIONS

The spatial and temporal patterns of cloud cover based on the QA MODIS daily imagery dataset over the Northeast region of Brazil was investigated in this study. The dataset provides the estimation of clear, cloudy and mixed conditions per pixel, during the period from 2000 to 2019. The results showed that the Amazon and Atlantic Forest biomes are the most strongly regions affected by clouds, with more than 60% of images classified as cloudy and mixed, while Caatinga and Cerrado biomes are less affected, with less than 45% of images. The most favorable months for the acquisition of optical sensor in orbital images were from May to October, characterized by the dry season, especially in Cerrado biome. The wet season (November – April) affects directly the image acquisitions, reducing to most than a half of cloud-free images in the Amazon, Caatinga, and Cerrado biomes.

Although the spatial resolution of the MOD09GA product is low, the daily temporal resolution increases the probability of finding pixels without the incidence of clouds, providing a general distribution in the NEB. Efforts that require more frequent observations and higher spatial resolutions for better land cover monitoring, may be restricted using a single-class sensor dataset (e.g. Landsat), once the lower temporal resolution the lower probability of finding cloud-free images. In this manner, independently of the sensor used, it is highly recommended to know, a priori, the spatial and temporal distribution of cloud cover derived from orbital images of the study area in order to plan monitoring efforts.

Referências

ACKER, J.G.; LEPTOUKH, G. Online analysis enhances use of NASA earth science data. **Eos. Transactions American Geophysical Union**, 88(2), pp.14-17, 2007. DOI. 10.1029/2007EO020003.

ACKERMAN, S.A.; STRABALA, K.I.; MENZEL, W.P.; FREY, R.A.; MOELLER, C.C.; GUMLEY, L.E. Discriminating clear sky from clouds with MODIS. **Journal of Geophysical Research:** Atmospheres, 103(D24), pp.32141-32157, 1998. DOI. 10.1029/1998JD200032.

ALVARES, C.A.; STAPE, J.L.; SENTELHAS, P. C.; GONÇALVES, J. L. M. Modeling monthly mean air temperature for Brazil. **Theoretical and Applied Climatolology**, v.113, p.407–427, 2013. DOI. 10.1007/s00704-012-0796-6.

ARAGÃO, L.E.O.C.; ANDERSON, L.O.; FONSECA M.G.; ROSAN, T.M.; VEDOVATO, L.B.; WAGNER, F.H.; SILVA, C.V.J.; JUNIOR, C.H.L.S.; ARAI, E.; AGUIAR, A.P.; BARLOW, J.; BERENGUER, E.; DEETER, M.N.; DOMINGUES, L.G.; GATTI, L.; GLOOR, M.; MALHI, Y.; MARENGO, J.A.; MILLER, J.B.; PHILLIPS, O. L.; SAATCHI, S. 21st century drought-related fires counteract the decline of Amazon deforestation carbon emissions. **Nature Communications**, 9:536, p. 1-12, 2018. DOI. 10.1038/s41467-017-02771-y.

ASNER, G.P. Cloud cover in Landsat observations of the Brazilian Amazon. **International Journal of Remote Sensing**, 22(18), pp.3855-3862, 2001. DOI. 10.1080/01431160010006926.

ASSIS, L. F. F. G.; FERREIRA, K. R.; VINHAS, L.; MAURANO, L.; ALMEIDA, C.; CARVALHO, A.; RODRIGUES, J.; MACIEL, A.; CAMARGO, C. TerraBrasilis: A Spatial Data Analytics Infrastructure for Large-Scale Thematic Mapping. **ISPRS International Journal of Geo-Information**, 8, 513, 2019. DOI. 10.3390/ijgi8110513.

BARBOSA, H.A., KUMAR, T.L., PAREDES, F., ELLIOTT, S.; AYUGA, J.G. Assessment of Caatinga response to drought using meteosat-SEVIRI normalized difference vegetation index (2008–2016). **ISPRS Journal of Photogrammetry and Remote Sensing**, 148, pp.235-252, 2019. DOI. 10.1016/j.isprsjprs.2018.12.014.

BORGES, E.F.; SANO, E.E. Temporal series of EVI from MODIS sensor for land use and land cover mapping of western Bahia. **Boletim de Ciencias Geodesicas**, 20(3), pp.526-547, 2014. DOI. 10.1590/S1982-21702014000200030.

BRANDT, M.; HIERNAUX, P.; RASMUSSEN, K.; MBOW, C.; KERGOAT, L.; TAGESSON, T.; IBRAHIM, Y.Z.; WÉLÉ, A.; TUCKER, C.J.; FENSHOLT, R. Assessing woody vegetation trends in Sahelian drylands using MODIS based seasonal metrics. **Remote Sensing of Environment**, 183, pp.215-225, 2016. DOI. 10.1016/j.rse.2016.05.027.

BRAZILIAN INSTITUTE OF GEOGRAPHY AND STATISTICS (IBGE). **Bases Cartográficas Contínuas,** 2016. Available in: <https://www.ibge.gov.br/geociencias/cartas-e-mapas/bases-cartograficas-continuas/15759 brasil.html?=&t=acesso-ao-produto>. Accessed in: may 2018.

BRITO, S.S.B., CUNHA, A.P.M., CUNNINGHAM, C.C., ALVALÁ, R.C., MARENGO, J.A. AND CARVALHO, M.A. Frequency, duration and severity of drought in the Semiarid Northeast Brazil region. **International Journal of Climatology**, 38(2), pp.517-529, 2018. DOI. 10.1002/joc.5225.

CASSOL, H.L.G., ARAI, E., SANO, E.E., DUTRA, A.C., HOFFMANN, T.B. AND SHIMABUKURO, Y.E. Maximum Fraction Images Derived from Year-Based Project for On-Board Autonomy-Vegetation (PROBA-V) Data for the Rapid Assessment of Land Use and Land Cover Areas in Mato Grosso State, Brazil. **Land**, 9(5), pp.1-20, 2020. DOI. 10.3390/land9050139.

CLAVERIE, M., JU, J., MASEK, J.G., DUNGAN, J.L., VERMOTE, E.F., ROGER, J.C., SKAKUN, S.V.; JUSTICE, C. The Harmonized Landsat and Sentinel-2 surface reflectance data set. **Remote Sensing of Environment**, 219, pp.145-161, 2018. DOI. 10.1016/j.rse.2018.09.002.

CONFALONIERI, U.E.; LIMA, A.C.L.; BRITO, I.; QUINTÃO, A.F. Social, environmental and health vulnerability to climate change in the Brazilian Northeastern Region. **Climatic Change**, 127(1), pp.123-137, 2014. DOI. 10.1007/s10584-013-0811-7.

COLUZZI, R.; IMBRENDA, V.; LANFREDI, M.; SIMONIELLO, T. A first assessment of the Sentinel-2 Level 1-C cloud mask product to support informed surface analyses. **Remote Sensing of Environment**, 217, pp.426-443, 2018. DOI. 10.1016/j.rse.2018.08.009.

CUNHA, A.P.M.; TOMASELLA, J.; RIBEIRO-NETO, G.G.; BROWN, M.; GARCIA, S.R.; BRITO, S.B.; CARVALHO, M.A. Changes in the spatial–temporal patterns of droughts in the Brazilian Northeast.

Atmospheric Science Letters, 19(10), p.e855, 2018. DOI. 10.1002/asl.855.

CUNHA, A.P.M.; ALVALÁ, R.C.; NOBRE, C.A.; CARVALHO, M.A. Monitoring vegetative drought dynamics in the Brazilian semiarid region. **Agricultural and Forest Meteorology**, 214, pp.494-505, 2015. DOI. 10.1016/j.agrformet.2015.09.010.

DA SILVA, P.F.; DE SOUSA LIMA, J.R.; ANTONINO, A.C.D.; SOUZA, R.; DE SOUZA, E.S.; SILVA, J.R.I.; ALVES, E.M. Seasonal patterns of carbon dioxide, water and energy fluxes over the Caatinga and grassland in the semi-arid region of Brazil. **Journal of Arid Environments**, 147, pp.71-82, 2017. DOI. 10.1016/j.jaridenv.2017.09.003.

DE ALBUQUERQUE, U.P.; DE LIMA ARAÚJO, E.; EL-DEIR, A.C.A.; DE LIMA, A.L.A.; SOUTO, A.; BEZERRA, B.M.; FERRAZ, E.M.N.; FREIRE, E.M.X; SAMPAIO, E.V.D.S.B.; LAS-CASAS, F.M.G.; DE MOURA, G.J.B.; Caatinga revisited: ecology and conservation of an important seasonal dry forest. **The Scientific World Journal**, 2012. DOI. 10.1100/2012/205182.

DIDAN, K.; MUNOZ, A.B.; SOLANO, R.; HUETE, A. **MODIS vegetation index user's guide (MOD13 series)**. Tucson: The University of Arizona, p.1-38, 2015. Available in: < https://vip.arizona.edu/documents/MODIS/MODIS_VI_UsersGuide_June_2015_C6.pdf>. Accessed in: dec. 2019.

DOS SANTOS, C.A.; MARIANO, D.A.; NASCIMENTO, F.C.A.; DANTAS, F.R.D.C.; DE OLIVEIRA, G.; SILVA, M.T.; DA SILVA, L.L.; DA SILVA, B.B.; BEZERRA, B.G.; SAFA, B.; MEDEIROS, S.D.S. Spatio-temporal patterns of energy exchange and evapotranspiration during an intense drought for drylands in Brazil. **International Journal of Applied Earth Observation and Geoinformation**, 85, p.101982, 2020. DOI. 10.1016/j.jag.2019.101982.

DRUSCH, M.; DEL BELLO, U.; CARLIER, S.; COLIN, O.; FERNANDEZ, V.; GASCON, F.; HOERSCH, B.; ISOLA, C.; LABERINTI, P.; MARTIMORT, P.; MEYGRET, A.; SPOTO, F.; SY, O.; MARCHESE, F.; BARGELLINI, P. Sentinel-2: ESA's optical high-resolution mission for GMES operational services. **Remote Sensing of Environment,** 120, 25–36, 2012. DOI. 10.1016/j.rse.2011.11.026.

GORELICK, N.; HANCHER, M.; DIXON, M.; ILYUSHCHENKO, S.; THAU, D.; MOORE, R. Google Earth Engine: planetary-scale geospatial analysis for everyone. **Remote Sensing of Environment**, 202, 18–27, 2017. DOI. 10.1016/j.rse.2017.06.031.

HILKER, T.; WULDER, M.A.; COOPS, N.C.; LINKE, J.; MCDERMID, G.; MASEK, J.G.; GAO, F.; WHITE, J.C. A new data fusion model for high spatial-and temporal-resolution mapping of forest disturbance based on Landsat and MODIS. **Remote Sensing of Environment**, v. 113, n. 8, pp. 1613-1627, 2009. DOI. 10.1016/j.rse.2009.03.007.

JUSTICE, C.O.; TOWNSHEND, J.R.G.; VERMOTE, E.F.; MASUOKA, E.; WOLFE, R.E.; SALEOUS, N.; ROY, D.P.; MORISETTE, J.T. An overview of MODIS Land data processing and product status. **Remote Sensing of Environment**, 83(1-2), pp.3-15, 2002. DOI. 10.1016/S0034-4257(02)00084-6.

KOUSKY, V.E. Frontal influences on northeast Brazil. **Monthly Weather Review**, v.107, n.9, p.1140-1153, 1979. DOI. 10.1175/1520-0493(1979)107<1140:FIONB>2.0.CO;2.

KRAATZ, S.; KHANBILVARDI, R.; ROMANOV, P. A comparison of MODIS/VIIRS cloud masks over ice-bearing river: on achieving consistent cloud masking and improved river ice mapping. **Remote Sensing**, 9(3), p.229, 2017. DOI. 10.3390/rs9030229.

LAPOLA, D.M.; MARTINELLI, L.A.; PERES, C.A.; OMETTO, J.P.H.B.; FERREIRA, M.E.; NOBRE, C.A.; AGUIAR, A.P.D.; BUSTAMANTE, M.M.C.; CARDOSO, M.F.; COSTA, M.H.; JOLY, C.A.; LEITE, C.C.; MOUTINHO, P.; SAMPAIO, G.; STRASSBURG, B.B.N.; VIEIRA, I.C.G. Pervasive transition of the Brazilian land-use system. **Nature Climate Chang**e, 4, 27–35, 2014. doi:10.1038/nclimate2056. DOI. 10.1038/nclimate2056.

LI, J., ROY, D., A global analysis of Sentinel-2A, Sentinel-2B and Landsat-8 data revisit intervals and implications for terrestrial monitoring. **Remote Sensing**, 9, 902. 2017. DOI. 10.3390/rs9090902

LI, W.; BARET, F.; WEISS, M.; BUIS, S.; LACAZE, R.; DEMAREZ, V.; DEJOUX, J. FRANCOIS;

BATTUDE, M.; CAMACHO, F. Combining hectometric and decametric satellite observations to provide near real time decametric fapar product. **Remote Sensing of Environment**, v. 200, p. 250–262, 2017. DOI. 10.1016/j.rse.2017.08.018.

LU, X.; LIU, R.; LIU, J.; LIANG, S. Removal of Noise by Wavelet Method to Generate High Quality Temporal Data of Terrestrial MODIS Products. **American Society for Photogrammetric Engineering & Remote Sensing**, v. 73, n. 10, p. 1129-1139, 2007. DOI. 10.14358/PERS.73.10.1129.

MAPBIOMAS. **Mapeamento Anual da Cobertura e Uso do Solo no Brasil**, 2020. Available in: <http://mapbiomas.org>. Accessed in: may 2020.

MARENGO, J.A.; CUNHA, A.P.; ALVES, L.M. A seca de 2012-15 no semiárido do Nordeste do Brasil no contexto histórico. Climanálise, v.3, p.1-6, 2016.

MARIANO, D.A.; DOS SANTOS, C.A.; WARDLOW, B.D.; ANDERSON, M.C.; SCHILTMEYER, A.V.; TADESSE, T.; SVOBODA, M.D. Use of remote sensing indicators to assess effects of drought and human-induced land degradation on ecosystem health in Northeastern Brazil. **Remote Sensing of Environment**, 213, pp.129-143, 2018. DOI. 10.1016/j.rse.2018.04.048.

MOLION, L.C.B.; BERNARDO, S.O. Uma revisão da dinâmica das chuvas no nordeste brasileiro. **Revista Brasileira de Meteorologia**, v.17, p.1-10, 2002.

NATIONAL INSTITUTE FOR SPACE RESEARCH (INPE), **Portal do Monitoramento de Queimadas e Incêndios**, 2018. Available in: <http://www.inpe.br/queimadas>. Accessed in: may 2020.

NATIONAL INSTITUTE FOR SPACE RESEARCH (INPE). Coordenação Geral de Observação da Terra. **Programa de Monitoramento da Amazônia e Demais Biomas. Desmatamento – Amazônia Legal**. Available in: <http://terrabrasilis.dpi.inpe.br/downloads/>. Accessed in: may 2020.

NATIONAL INSTITUTE FOR SEMIARID (INSA). **Portal do Instituto Nacional do Semiárido**. Available in: <https://portal.insa.gov.br/>. Accessed in: may 2020.

PALHARINI, A.; SANTOS, R.; VILA, D.A. Climatological behavior of precipitating clouds in the northeast region of Brazil. **Advances in Meteorology**, 5916150, 2017. DOI. 10.1155/2017/5916150.

PARENTE, L.; MESQUITA, V.; MIZIARA, F.; BAUMANN, L.; FERREIRA, L. Assessing the pasturelands and livestock dynamics in Brazil, from 1985 to 2017: a novel approach based on high spatial resolution imagery and Google Earth Engine cloud computing. **Remote Sensing of Environment**, 232, 111301, 2019. DOI. 10.1016/j.rse.2019.111301.

R CORE TEAM. **R: A language and environment for statistical computing**. R Foundation for Statistical Computing, Vienna, Austria, 2020.

ROY, D.P.; BORAK, J.S.; DEVADIGA, S.; WOLFE, R.E.; ZHENG, M.; DESCLOITRES, J.; The MODIS land product quality assessment approach. **Remote Sensing of Environment**. 83, 62–76, 2002. DOI. 10.1016/S0034-4257(02)00087-1.

ROY, D.P.; HUANG, H; BOSCHETTI, L.; GIGLIO, L.; YAN, L.; ZHANG, H.H.; LI, Z. Landsat-8 and Sentinel-2 burned area mapping-A combined sensor multi-temporal change detection approach. **Remote Sensing of Environment**, 231, p.111254, 2019. DOI. 10.1016/j.rse.2019.111254.

RUDORFF, B.F.T.; AGUIAR, D.A.; SILVA, W.F.; SUGAWARA, L.M.; ADAMI, M.; MOREIRA, M.A. Studies on the rapid expansion of sugarcane for ethanol production in São Paulo State (Brazil) using Landsat data. **Remote Sensing**, v.2, p. 1057-1076, 2010. DOI. 10.3390/rs2041057.

SANO, E.E.; FERREIRA, L.G.; ASNER, G.P.; STEINKE, E.T. Spatial and temporal probabilities of obtaining cloud-free Landsat images over the Brazilian tropical savanna. **International Journal of Remote Sensing**, v.28, n.12, p.2739-2752, 2007. DOI. 10.1080/01431160600981517.

SANO, E.E.; ROSA, R.; BRITO, J.L.S.; FERREIRA, L.G. Land cover mapping of the tropical savanna region in Brazil. **Environmental Monitoring and Assessment**, 166, 113–124, 2010. DOI. 10.1007/s10661-009-0988-4.

SANTOS, J.C.; LEAL, I.R.; CORTEZ, J.S.A.; FERNANDES, G.W.; TABARELLI, M. Caatinga: the scientific negligence experienced by a dry tropical forest. **Tropical Conservation Science**, v.4, n.3, p.276-

286, 2011. DOI. 10.1177/194008291100400306.

SANTOS, J.R.N.; SILVA, F.B.; SILVA JUNIOR, C.H.L.; ARAÚJO, M.D. Precisão dos dados do satélite Tropical Rainfall Measuring Mission (TRMM) na região de transição Amazônia-Cerrado no Estado do Maranhão. In: XVII Simpósio Brasileiro de Sensoriamento, João Pessoa. **Anais...** João Pessoa: INPE, 2015.

SHIMABUKURO, Y. E.; SMITH, J. A. Fraction images derived from Landsat TM and MSS data for monitoring reforested areas. **Canadian Journal of Remote Sensing**, v. 21, n. 1, p. 67–74, 1995. DOI. 10.1080/07038992.1995.10874599.

SILVA, J.M.C.; LEAL, I.R.; TABARELLI, M. **Caatinga:** the largest tropical dry forest region in South America. Berlin: Springer, 2018.

SOARES, A.S.D.; PAZ, A.R.D.; PICCILLI, D.G.A. Avaliação das estimativas de chuva do satélite TRMM no Estado da Paraíba. **Revista Brasileira de Recursos Hídricos**, 21(2), pp.288-299, 2016. DOI. 10.21168/rbrh.v21n2.p288-299.

SOS MATA ALTÂNTICA FOUNDATION (SOSMA). **Atlas da Mata Atlântica**. Available in: <https://www.sosma.org.br/iniciativa/atlas-da-mata-atlantica>. Accessed in: may 2020.

TEAM, R. **RStudio: integrated development for R. RStudio**, Inc., Boston, MA. 42, p.14, 2015. Available in: <http://www.rstudio.com>. Accessed in: mar. 2018.

TOMASELLA, J.; VIEIRA, R.M.S.P.; BARBOSA, A.A.; RODRIGUEZ, D.A.; DE OLIVEIRA SANTANA, M.; SESTINI, M.F., Desertification trends in the Northeast of Brazil over the period 2000–2016. **International Journal of Applied Earth Observation and Geoinformation**, 73, pp.197-206, 2018. DOI. 10.1016/j.jag.2018.06.012.

TROPICAL RAINFALL MEASURING MISSION (TRMM). **TRMM (TMPA/3B43) Rainfall Estimate L3 1 month 0.25 degree x 0.25 degree V7**, Greenbelt, MD, Goddard Earth Sciences Data and Information Services Center (GES DISC), 2011. Available in: < https://disc.gsfc.nasa.gov/datasets/TRMM_3B43_7/summary>. Accessed in: oct. 2017. DOI.10.5067/TRMM/TMPA/MONTH/7.

VERMOTE, E.; WOLFE, R. **MOD09GA MODIS/Terra Surface Reflectance Daily L2G Global 1 km and 500m SIN Grid V006.** NASA EOSDIS Land Processes DAAC, 2015. Available in: < https://lpdaac.usgs.gov/products/mod09gav006/>. Accessed in: dec. 2019. DOI. 10.5067/MODIS/MOD09GA.006.

VIEIRA, R.M.D.S.P.; CUNHA, A.P.M.D.A.; ALVALÁ, R.C.D.S.; CARVALHO, V.C.; FERRAZ NETO, S.; SESTINI, M.F. Land use and land cover map of a semiarid region of Brazil for meteorological and climatic models. **Revista Brasileira de Meteorologia**, 28(2), pp.129-138, 2013. DOI. 10.1590/S0102-77862013000200002.

WOLFE, R.E.; ROY, D.P.; VERMOTE, E. MODIS land data storage, gridding, and compositing methodology: Level 2 grid. **IEEE Transactions on Geoscience and Remote Sensing**, vol. 36, no. 4, pp. 1324-1338, 1998. DOI. 10.1109/36.701082.

YOUSEF, L.A.; TEMIMI, M.; MOLINI, A.; WESTON, M.; WEHBE, Y.; AL MANDOUS, A. Cloud Cover over the Arabian Peninsula from Global Remote Sensing and Reanalysis Products. **Atmospheric Research**, 238, p.104866, 2020. DOI. 10.1016/j.atmosres.2020.104866.

ZALLES, V.; HANSEN, M.C.; POTAPOV, P.V.; STEHMAN, S.V.; TYUKAVINA, A.; PICKENS, A.; SONG, X.P.; ADUSEI, B.; OKPA, C.; AGUILAR, R.; JOHN, N. Near doubling of Brazil's intensive row crop area since 2000. **Proceedings of the National Academy of Sciences**, 116(2), pp.428-435, 2019. DOI. 10.1073/pnas.1810301115.

 DOI: http://dx.doi.org/10.14393/rbcvxxnx-xxxx

Aknowledgments

This research was funded by the CNPq (Brazilian National Council for Scientific and Technological Development), Process No. 303299/2018-5 and Process No. 134138/2018-0. The authors would like to thank the infrastructure provided by INPE (National Institute for Space Research) and the anonymous reviewers for their valuable comments and suggestions that greatly improved the quality of the technical and presentation form of the manuscript.

Authors Contribution

Andeise Dutra and Egidio Arai conceptualized and designed the research, as well performed data processing. Andeise Dutra performed the analysis, visualization, methodology execution and wrote the manuscript. Yosio Shimabukuro and Claudia Sampaio contributed to the manuscript revision and edition.

Conflicts of Interest

The authors declare no conflicts of interest.

Author's Biography

Andeise Cerqueira Dutra was born in Bahia State, Brazil. She received the BSc in Forestry Engineering from the Federal University of Recôncavo da Bahia (UFRB) in 2017 and the MSc in Remote Sensing from the National Institute for Space Research (INPE) in 2019. She is currently a fellowship from the National Council for Scientific and Technological Development (CNPq) on the project of the Cerrado biome fire risk system (SIRI). Her interests are species phenology, land-use and land-cover changes, and monitoring of vegetation over different biomes in Brazil using remote sensing and geographic information system techniques.